

# Soliton Random Walk and the Cluster-Stripping Problem in Ultralight Dark Matter

Hsi-Yu Schive (薛熙于)<sup>1,2,3,\*</sup> Tzihong Chiueh (闕志鴻)<sup>1,2,3</sup> and Tom Broadhurst<sup>4,5</sup>

<sup>1</sup>*Department of Physics, National Taiwan University, Taipei 10617, Taiwan*

<sup>2</sup>*Institute of Astrophysics, National Taiwan University, Taipei 10617, Taiwan*

<sup>3</sup>*Center for Theoretical Physics, National Taiwan University, Taipei 10617, Taiwan*

<sup>4</sup>*Department of Theoretical Physics, University of the Basque Country UPV/EHU, Bilbao, Spain*

<sup>5</sup>*Ikerbasque, Basque Foundation for Science, Bilbao, Spain*

(Dated: April 22, 2020)

Simulations of ultralight,  $\sim 10^{-22}$  eV, bosonic dark matter exhibit rich wave-like structure, including a soliton core within a surrounding halo that continuously self-interferes on the de Broglie scale. We show here that as an inherent consequence, the soliton undergoes a confined random walk at the base of the halo potential. This is significant for the fate of the ancient central star cluster in Eridanus II, as the agitated soliton gravitationally shakes the star cluster in and out of the soliton on a time scale of  $\sim 100$  Myr, so complete tidal disruption of the star cluster can occur within  $\sim 1$  Gyr. This destructive effect can be mitigated by tidal stripping of the halo of Eridanus II, thereby reducing the agitation, depending on its orbit around the Milky Way. Our simulations show the Milky Way tide affects the halo much more than the soliton, so the star cluster in Eridanus II can survive for over 5 Gyr within the soliton if it formed after significant halo stripping.

PACS numbers:

*Introduction.* A Bose-Einstein condensate of ultralight bosons with mass  $m \sim 10^{-22}$  eV has become a viable interpretation of dark matter (DM) [1–8], often termed fuzzy DM (FDM) or wave DM ( $\psi$ DM). This has the desirable effect of suppressing dwarf galaxies [9] as the uncertainty principle counters self-gravity below the de Broglie wavelength, and provides the same large-scale structure as the standard cold DM model [7, 10].

Pioneering  $\psi$ DM simulations have revealed pervasive, wave-like structure, with a soliton core at the base of every halo, surrounded by turbulent density fluctuations that self-interfere [7, 11]. The soliton is a prominent flat-topped overdensity comparing favorably with dwarf galaxies [7, 12–14] but in tension with the HI based smoothly rising rotation curves of more massive galaxies [14–16]. The ambient density fluctuations are fully modulated, which may measurably heat stars [17–20]. Direct Compton scale oscillations for pulsars residing within dense solitons may also be detectable [21].

The existence of a central star cluster in the ultrafaint dwarf galaxy Eridanus II (Eri II) provides a unique probe for constraining DM models [22]. It has been suggested that the gravitational heating from the oscillations of soliton peak density should destroy the star cluster completely for  $10^{-21}$  eV  $\lesssim m \lesssim 10^{-19}$  eV [23]. In this Letter, using self-consistent  $\psi$ DM simulations, we show that the central soliton exhibits random-walk behavior, which can lead to complete tidal disruption of the star cluster within  $\sim 1$  Gyr even for  $m \sim 10^{-22}$  eV. This problem is distinctly different and potentially more serious than the gravitational heating problem above.

*Simulation setup.* We follow the evolution of a star cluster embedded in the center of a  $\psi$ DM halo mimicking Eri II. For the halo component, we extract it from a cosmological simulation [11] at redshift zero, with

a virial mass of  $M_{\text{vir}} \sim 6 \times 10^9 M_{\odot}$  and a radius of  $r_{\text{vir}} \sim 50$  kpc. It hosts a soliton with a half-density radius of  $r_{\text{sol}} \sim 0.7$  kpc, an enclosed mass within  $r_{\text{sol}}$  of  $M_{\text{sol}} \sim 1 \times 10^8 M_{\odot}$ , and a peak density of  $\rho_{\text{sol}} \sim 3 \times 10^6 \bar{\rho}_{\text{DM}} \sim 0.1 M_{\odot} \text{pc}^{-3}$  where  $\bar{\rho}_{\text{DM}} \sim 4 \times 10^{-8} M_{\odot} \text{pc}^{-3}$  represents the mean DM density. The mass within 280 pc is  $\sim 1 \times 10^7 M_{\odot}$ , consistent with Eri II that has a mass of  $M_{1/2} = 1.2_{-0.3}^{+0.4} \times 10^7 M_{\odot}$  within a half-light radius of  $r_{1/2} = 277 \pm 14$  pc (corresponding to a velocity dispersion of  $6.9 \text{ km s}^{-1}$ ) [24].

The central star cluster in Eri II has a mass of  $M_{\text{EII}} \sim 2 \times 10^3 M_{\odot}$ , a half-light radius of  $r_{\text{EII}} \sim 13$  pc, an age of  $T_{\text{EII}} \gtrsim 3$  Gyr, and a very shallow density profile [24, 25]. We model it by a Plummer sphere with a peak stellar mass density of  $\rho_{*,\text{max}} \sim 0.2 M_{\odot} \text{pc}^{-3}$  and a scale radius of  $\sim 20$  pc. It corresponds to an enclosed mass within  $r_{\text{EII}}$  of  $\sim 1 \times 10^3 M_{\odot}$ , consistent with observations. The star cluster is self-bound since  $\rho_{*,\text{max}} > \rho_{\text{sol}}$  and its center coincides with the soliton center initially.

The governing equation of  $\psi$ DM is the Schrödinger-Poisson equation [2],

$$\left[ i \frac{\hbar}{m} \frac{\partial}{\partial t} + \frac{\hbar^2}{2m^2} \nabla^2 - V_{\psi} \right] \psi = 0, \quad (1)$$

$$\nabla^2 V_{\psi} = 4\pi G m |\psi|^2, \quad (2)$$

where  $\psi$  is the wave function,  $V_{\psi}$  is the gravitational potential,  $\hbar$  is the reduced Planck constant, and  $G$  is the gravitational constant.  $\rho_{\text{DM}} = m |\psi|^2$  gives the DM mass density. We adopt  $m = 8 \times 10^{-23}$  eV throughout this work to be consistent with [7, 11].

To evolve  $\psi$ DM and stars, we use the code GAMER [26], which supports adaptive mesh refinement with hybrid parallelization. It employs an explicit second-order

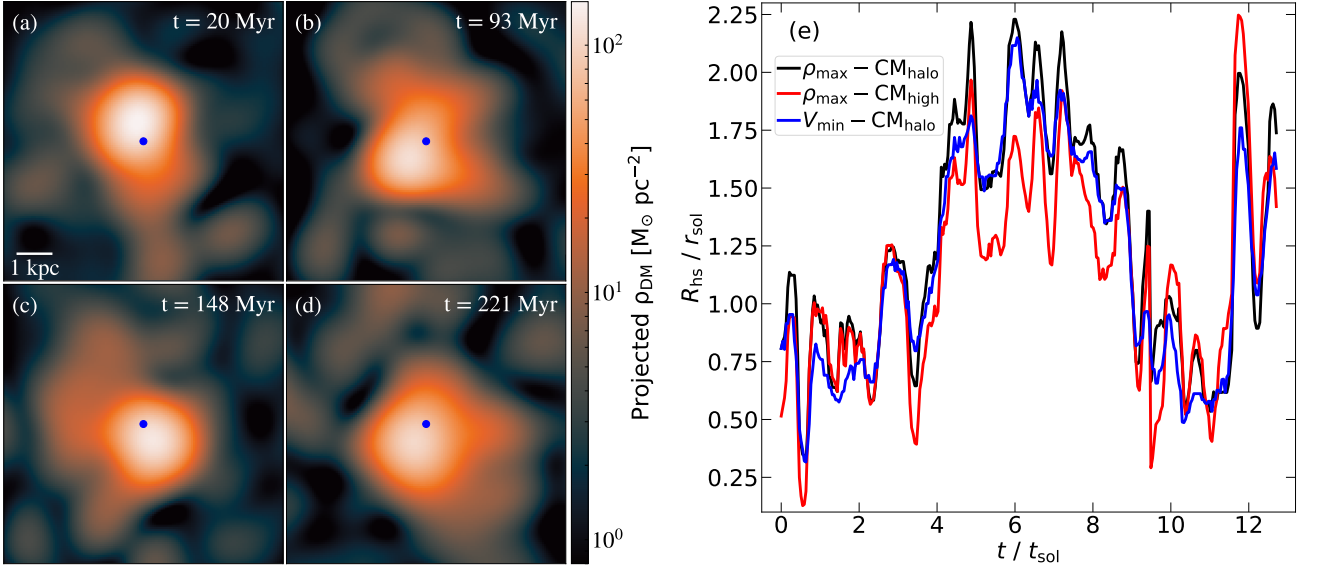


FIG. 1: Soliton random walk. (a)–(d) Projected DM density in a 4 kpc thick slab centered on the halo center of mass (CM<sub>halo</sub>; filled circle). Bright region (with a surface density  $\gtrsim 50 \text{ M}_\odot \text{ pc}^{-2}$ ) represents the soliton. Offset between the halo and soliton centers is manifest and constantly changing. (e) Separation between the halo and soliton centers ( $R_{\text{hs}}$ ) as a function of time, normalized to the characteristic length scale ( $r_{\text{sol}} \sim 0.7 \text{ kpc}$ ) and time scale ( $t_{\text{sol}} \sim 1 \times 10^2 \text{ Myr}$ ) of the soliton. Soliton random motion exhibits similar length and time scales as  $r_{\text{sol}}$  and  $t_{\text{sol}}$ , respectively. These results are insensitive to the specific definitions of centers, which we demonstrate with four different choices: (i) CM<sub>halo</sub>, (ii) CM of high-density regions with  $\rho_{\text{DM}} > 10^4 \bar{\rho}_{\text{DM}}$  (CM<sub>high</sub>), (iii) positions of the soliton peak density ( $\rho_{\text{max}}$ ), and (iv) potential minimum ( $V_{\text{min}}$ ). The latter two closely follow each other due to the massive compact soliton.

finite-difference method to solve Eqs. (1) and (2) [7] and has been extensively applied to  $\psi$ DM simulations (e.g., [7, 11, 27]).

We simulate a volume of size  $L = 250 \text{ kpc}$ , with a root grid  $N = 128^3$  and up to nine refinement levels. To resolve the  $\psi$ DM halo and soliton, cells with  $\rho_{\text{DM}} > 10^l \bar{\rho}_{\text{DM}}$  are refined to level  $l + 1$  for  $0 \leq l \leq 3$ , leading to a resolution of  $0.12 \text{ kpc} \sim (1/6)r_{\text{sol}}$ . Furthermore, to resolve the central star cluster, grid patches (each with  $8^3$  cells) containing more than  $10^3$  particles are refined, giving a maximum resolution of  $3.8 \text{ pc} \lesssim (1/3)r_{\text{EII}}$ . This high resolution makes time-steps as small as  $\Delta t \sim 150 \text{ yr}$  due to the stringent Courant-Friedrichs-Lewy condition imposed by Eq. (1). The total number of collisionless particles for sampling the star cluster is  $2 \times 10^5$ , corresponding to a particle mass resolution of  $3.6 \times 10^{-2} \text{ M}_\odot$ . We adopt isolated boundary conditions for gravity and sponge boundary conditions for wave function. We have validated the numerical convergence of all the presented results by adjusting the spatial resolution by up to a factor of 4 and the particle mass resolution by a factor of 10. We have also confirmed that an isolated star cluster without a  $\psi$ DM halo is stable over a Hubble time in our simulations.

*Isolated  $\psi$ DM halo.* We start by simulating an *isolated* system by ignoring the tidal field of the Milky Way. Fig. 1 shows the motion of the central soliton,

revealing a confined Brownian (random-walk-like) motion at the base of the halo potential. This random motion exhibits a characteristic length scale similar to the soliton radius  $r_{\text{sol}}$  and a time scale comparable to the oscillation period of the soliton wave function,  $t_{\text{sol}} \sim 120(\rho_{\text{sol}}/0.1 \text{ M}_\odot \text{ pc}^{-3})^{-1/2} \text{ Myr} \sim 120 \text{ Myr}$ . These results are insensitive to the definitions of halo and soliton centers (as shown in Fig. 1), and the drift of the halo center of mass caused by numerical errors is found to be of order  $10^{-2}r_{\text{sol}}$ , indicating that this soliton random motion is not a numerical artifact.

The star cluster can be treated as a tracer of the soliton as the latter is five orders of magnitude more massive. The characteristic free-fall time of a star cluster located just outside the soliton is  $t_{\text{ff}} \sim (G\rho_{\text{sol}})^{-1/2} \sim 50 \text{ Myr}$ , smaller but comparable to  $t_{\text{sol}}$ . It suggests that the star cluster can only loosely trace the random motion of soliton, resulting in a maximum separation between them, denoted as  $R_{\text{cs}}$ , of order  $r_{\text{sol}}$ . Fig. 2(a)–(d) illustrates this feature.

This large separation can have a great impact on the survival of the star cluster due to tidal stripping, as shown below. The soliton density profile features a flat core within  $\sim r_{\text{sol}}$  and a steep outer gradient. So, for  $R_{\text{cs}} > r_{\text{sol}}$ , a star at a distance  $r_*$  to the star cluster center will be subject to a tidal field  $f_{\text{tidal}} \sim 2GM_{\text{sol}}r_*/R_{\text{cs}}^3 \propto R_{\text{cs}}^{-3}$ , assuming  $r_* \ll R_{\text{cs}}$ . For  $R_{\text{cs}} < r_{\text{sol}}$ , the star cluster

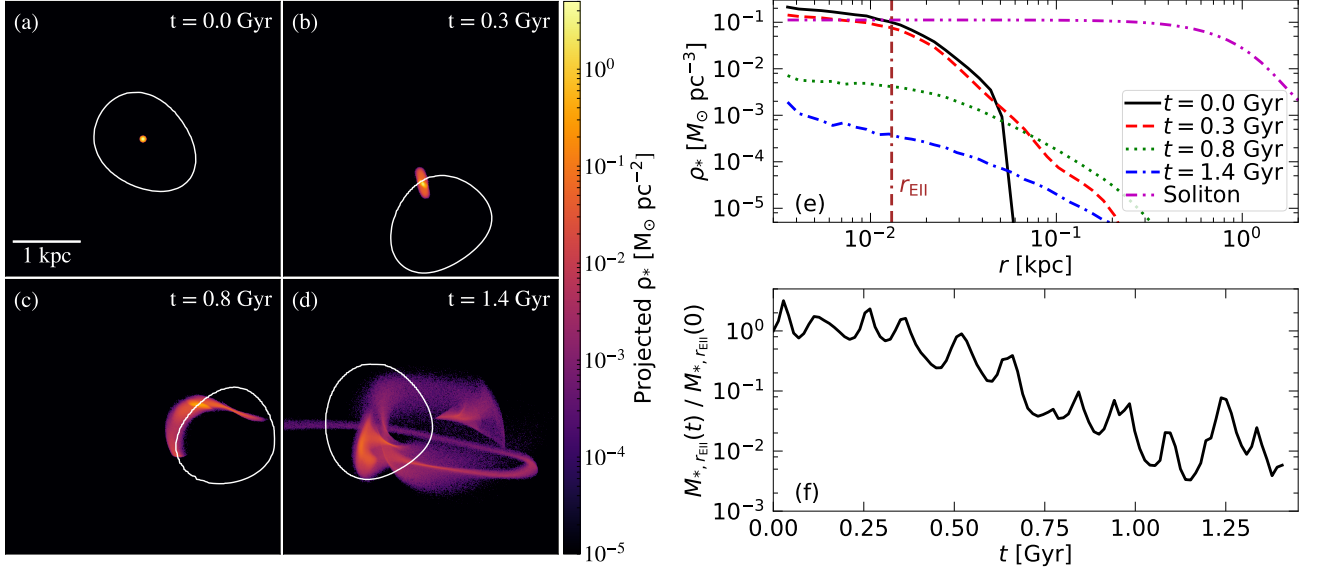


FIG. 2: Tidal stripping of a star cluster caused by soliton random walk. (a)–(d) Projected stellar mass density in a 4 kpc thick slab centered on the initial center of the star cluster. Contours indicate the soliton boundaries ( $\sim r_{\text{sol}}$ ) where the DM density drops by half. Although the star cluster and soliton centers coincide at the beginning by design, the soliton random motion quickly results in a separation between them of order  $r_{\text{sol}}$ , leading to a large tidal field that disrupts the star cluster (see text for details). (e) Stellar density profiles. The dash-double-dot line shows a soliton profile for comparison. The vertical (dash-dash-dot) line indicates the half-light radius ( $r_{\text{EII}}$ ) of the central star cluster in Eri II. (f) Enclosed stellar mass within  $r_{\text{EII}}$  as a function of time, normalized to its initial value. The star cluster loses  $\sim 99\%$  of its original mass after  $\sim 1$  Gyr.

will be compressed instead of tidally stripped. Therefore, tidal stripping is most effective when  $R_{\text{cs}} \sim r_{\text{sol}}$ , which is exactly what happens here. We can assess the significance of the tidal field at  $r_*$  by computing the ratio of  $f_{\text{tidal}}$  to the star cluster self-gravity  $f_*$ ,

$$\frac{f_{\text{tidal}}}{f_*} \simeq \frac{3}{2\pi} \frac{M_{\text{sol}}}{\rho_{*,\text{max}} R_{\text{cs}}^3} \simeq 2 \frac{\rho_{\text{sol}}}{\rho_{*,\text{max}}} \simeq \mathcal{O}(1), \quad (3)$$

where  $\rho_{\text{sol}} \sim 0.1 M_{\odot} \text{ pc}^{-3}$  and  $\rho_{*,\text{max}} \sim 0.2 M_{\odot} \text{ pc}^{-3}$  as described earlier. The fact that this ratio is of order unity and independent of  $r_*$  suggests that the entire star cluster is marginally stable and vulnerable to tidal disruption after  $t \gg t_{\text{ff}}$ .

This expectation is confirmed in Fig. 2(e) and (f), showing that the star cluster loses  $\sim 90\%$  and  $99\%$  of its original mass within  $r_{\text{EII}}$  after  $\sim 0.7$  and  $1$  Gyr, respectively. This disruption time scale is noticeably shorter than  $T_{\text{EII}}$  and can potentially present a serious challenge for  $\psi$ DM, which we refer to as the *cluster-stripping* problem. Nevertheless, in the following, we shall further show how the Milky Way tides may alleviate this problem by reducing the halo agitation of the soliton.

*Tidally disrupted  $\psi$ DM halo.* Satellite galaxies of the Milky Way are subject to its tidal field. Eri II, although currently at a Galactocentric distance of  $\sim 370$  kpc, may be on its second or third orbit around the Milky Way with an infall time of  $\sim 4 - 10$  Gyr ago and a periapsis of  $\sim 100 - 200$  kpc [24]. The question naturally arises

as to whether the Milky Way tides can affect the soliton random motion, and thus the survival of the central star cluster in Eri II.

Modeling the exact tidal stripping process of Eri II requires detailed information about its orbital parameters, which unfortunately still suffers from large uncertainties [28, 29]. As a proof-of-concept study, we adopt a circular orbit of radius  $R_{\text{MW}} = 100$  kpc for the satellite galaxy and a point mass of  $M_{\text{MW}} = 1 \times 10^{12} M_{\odot}$  to approximate the tidal field of the Milky Way. To speed up the simulations, we choose a moving non-rotating coordinate system, with the Milky Way center orbiting the coordinate origin that coincides with the center of mass of the satellite halo, in order to get rid of the small wavelength in  $\psi$  associated with the high orbital velocity. Assuming  $r \ll R_{\text{MW}}$ , where  $\mathbf{r}$  and  $\mathbf{R}_{\text{MW}}(t)$  are the position vectors of a simulation cell and the Milky Way center, respectively, the tidal potential can be approximated as

$$V_{\text{tidal}}(\mathbf{r}, t) \simeq \frac{GM_{\text{MW}}}{2R_{\text{MW}}^3} \left[ r^2 - 3 \left( \frac{\mathbf{r} \cdot \mathbf{R}_{\text{MW}}(t)}{R_{\text{MW}}} \right)^2 \right]. \quad (4)$$

The total potential is given by  $V_{\text{tot}} = V_{\psi} + V_{\text{tidal}}$ . We evolve the system for 9 Gyr.

Fig. 3 shows the tidal stripping process of a satellite halo. The halo surrounding the central soliton is found to be vulnerable to tidal disruption; the density at  $r \gtrsim 3r_{\text{sol}}$  decreases by more than an order of magnitude after  $\sim 2$  Gyr. In comparison, the soliton, which

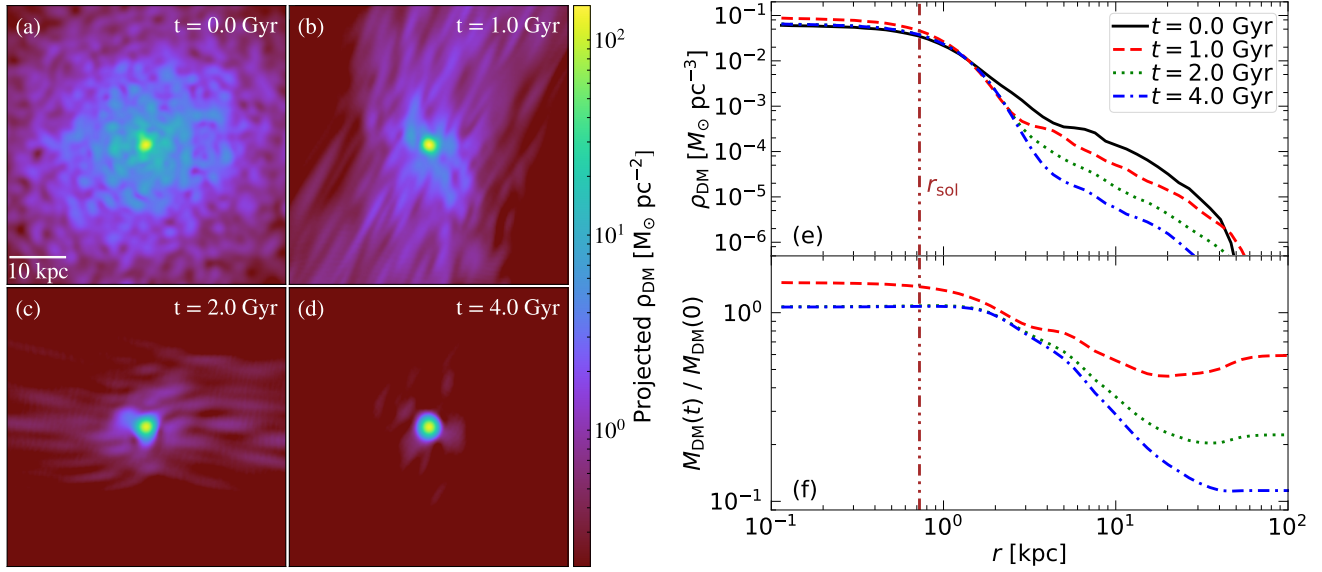


FIG. 3:  $\psi$ DM halo subject to the tidal field of the Milky Way. The halo has a circular orbit of radius 100 kpc and a period of  $\sim 3$  Gyr. (a)–(d) Projected DM density in a 50 kpc thick slab centered on the soliton (bright region with a surface density  $\gtrsim 50 M_\odot \text{ pc}^{-2}$ ). (e) Halo density profiles. (f) Halo enclosed mass profiles normalized to the initial profile. The vertical (dash-double-dot) line indicates the soliton radius  $r_{\text{sol}}$ . The soliton remains intact during the entire simulation period (9 Gyr) while the outer region ( $r \gtrsim 3 r_{\text{sol}}$ ) is tidally disrupted after a few Gyr.

is strongly gravitationally bound, is resilient to tidal disruption and stays intact during the entire simulation period, which ensures consistency with the observational constraint  $M_{1/2} \sim 1 \times 10^7 M_\odot$ .

During the tidal stripping of the halo, the soliton random motion is significantly diminished. Fig. 4(a) shows the separation between the halo and soliton centers as a function of time, where we define the halo center as the center of mass of high-density regions ( $\rho_{\text{DM}} > 10^4 \bar{\rho}_{\text{DM}}$ ) to exclude the stripped material. The separation, normalized to  $r_{\text{sol}}$ , reduces from  $\mathcal{O}(1)$  to  $\mathcal{O}(10^{-2})$  after  $\sim 5$  Gyr. This result is not surprising given that the soliton becomes increasingly dominant as the halo is being stripped.

In Fig. 4(b), we assess how the above findings affect the cluster-stripping problem by conducting four simulations and in each of them, we add the central star cluster at a different epoch,  $t_0 = 0, 2, 3, 4$  Gyr. We find that the later the star cluster is added, the more stable it is, because the tidal field induced by soliton random motion becomes weaker over time. For  $t_0 = 0$ , the result is almost identical to the case without considering the Milky Way tides (see Fig. 2) since the tidal disruption time scale of the star cluster ( $\lesssim 1$  Gyr) is shorter than that of the halo ( $\sim 2 - 4$  Gyr). In comparison, for  $t_0 = 4$  Gyr, at which the ambient medium of soliton has been largely stripped away (see Fig. 3), the star cluster can stay intact throughout the remaining simulation time in 5 Gyr. This period is longer than  $T_{\text{EII}}$  and thus free of the cluster-stripping problem.

*Concluding remarks.* We have reported a cluster-stripping problem specific to dwarf galaxy-sized  $\psi$ DM halos hosting a central star cluster, such as Eri II. Our unprecedentedly high-resolution simulations reveal, for the first time, random-walk-like behavior in the soliton core. This can displace the star cluster slightly outside the soliton radius ( $r_{\text{sol}}$ ), leading to efficient disruption of the star cluster due to the soliton tidal field.

As a possible solution, we have further demonstrated that if Eri II is bound to the Milky Way, the tidal field of the Milky Way may readily disrupt the outer part of a  $\psi$ DM subhalo, leaving the relatively dense soliton intact. In this case, the amplitude of soliton random motion declines significantly, and so a star cluster forming centrally after substantial halo removal can survive much longer. More accurate proper motion measurements of Eri II in the future will help clarify this possibility.

We emphasize that the  $\psi$ DM halo adopted here, which is consistent with the average DM density of Eri II, is directly extracted from a cosmological simulation with  $m \sim 1 \times 10^{-22}$  eV [11]. Therefore, it appears to undermine the claim that Eri II cannot form for  $m \lesssim 8 \times 10^{-22}$  eV based on the subhalo mass function [23], which likely underestimates the total halo mass by one to two orders of magnitude compared to our simulations. Our study also confirms that the star cluster heating due to the oscillations of soliton peak density is irrelevant for  $m \sim 1 \times 10^{-22}$  eV [23].

The soliton peak density scales as  $\rho_{\text{sol}} \propto m^{-2} r_{\text{sol}}^{-4}$  [11] and we adopt  $r_{\text{sol}} > r_{1/2}$ ,  $\rho_{\text{sol}} \sim \rho_{*,\text{max}}$ , and  $m = 8 \times$

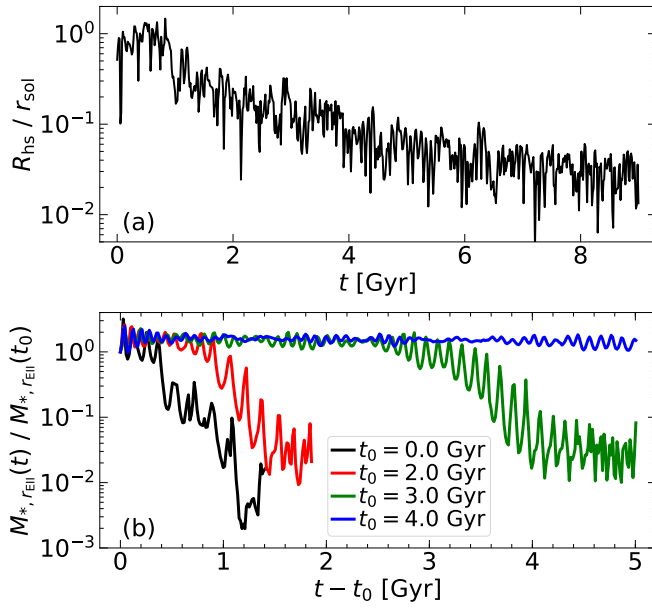


FIG. 4: Soliton random walk and the resulting tidal stripping of a central star cluster under the influence of the *Milky Way* potential. (a) Separation between the halo and soliton centers due to soliton random walk, similar to Fig. 1(e). The amplitude of random motion declines significantly as the halo being tidally disrupted by the Milky Way tides (see Fig. 3). (b) Enclosed stellar mass within  $r_{\text{EII}}$  normalized to its initial value, similar to Fig. 2(f). We add a star cluster at four different epochs ( $t_0$ ). For each case, the horizontal axis is shifted by  $t_0$  for better comparison. Clearly, the later the star cluster is added, the more stable it is, because the random motion becomes smaller over time and so does the induced tidal field. For  $t_0 = 4$  Gyr, the star cluster can remain intact for more than 5 Gyr, longer than the estimated minimum age of the central star cluster in Eri II ( $\sim 3$  Gyr), thus evading the cluster-stripping problem.

$10^{-23}$  eV. For  $m \lesssim 5 \times 10^{-22}$  eV, a soliton of a fixed  $\rho_{\text{sol}}$  can still satisfy the constraint  $M_{1/2} \sim 1 \times 10^7 M_{\odot}$  since  $r_{\text{sol}} \gtrsim r_{1/2}$ . So the tidal field remains roughly the same (Eq. (3)). For even larger  $m$ ,  $r_{\text{sol}} < r_{1/2}$  with a fixed  $\rho_{\text{sol}}$  and thus  $\rho_{\text{sol}}$  must increase, resulting in more efficient tidal stripping assuming the amplitude of random motion remains  $\sim r_{\text{sol}}$ .

To test  $\psi$ DM using solitons, it would be important to consider its random motion reported here. Examples include the dynamical friction and core stalling in dwarf galaxies [8, 30, 31], the galactic rotation curves [14–16], and the excess mass in the Milky Way center [32–34]. But it remains to be investigated how soliton random walk changes with halo mass.

*Acknowledgements.* We thank Frank van den Bosch and Zhi Li for insightful discussions. This research is partially supported by the Ministry of Science and Technology (MOST) of Taiwan under the grant No. MOST 107-2119-M-002-036-MY3 and MOST 108-2112-M-002-023-MY3, and the NTU Core Consortium project un-

der the grant No. NTU-CC-108L893401 and NTU-CC-108L893402. H.S. acknowledges the funding support from the Jade Mountain Young Scholar Award No. NTU-108V0201, sponsored by the Ministry of Education, Taiwan.

\* Electronic address: hyschive@phys.ntu.edu.tw

- [1] L. M. Widrow and N. Kaiser, *Astrophys. J. Lett.* **416**, L71 (1993).
- [2] W. Hu, R. Barkana, and A. Gruzinov, *Phys. Rev. Lett.* **85**, 1158 (2000), astro-ph/0003365.
- [3] P. J. E. Peebles, *Astrophys. J. Lett.* **534**, L127 (2000), astro-ph/0002495.
- [4] J. Goodman, *New Astron.* **5**, 103 (2000), astro-ph/0003018.
- [5] T. Matos and L. Arturo Ureña-López, *Phys. Rev. D* **63**, 063506 (2001), astro-ph/0006024.
- [6] D. J. E. Marsh, *Phys. Rep.* **643**, 1 (2016), 1510.07633.
- [7] H.-Y. Schive, T. Chiueh, and T. Broadhurst, *Nature Physics* **10**, 496 (2014), 1406.6586, (SCB14a).
- [8] L. Hui, J. P. Ostriker, S. Tremaine, and E. Witten, *Phys. Rev. D* **95**, 043541 (2017), 1610.08297.
- [9] J. S. Bullock and M. Boylan-Kolchin, *Annu. Rev. Astron. Astrophys.* **55**, 343 (2017), 1707.04256.
- [10] D. J. E. Marsh and J. Silk, *Mon. Not. R. Astron. Soc.* **437**, 2652 (2014), 1307.1705.
- [11] H.-Y. Schive *et al.*, *Phys. Rev. Lett.* **113**, 261302 (2014), 1407.7762, (S14b).
- [12] E. Calabrese and D. N. Spergel, *Mon. Not. R. Astron. Soc.* **460**, 4397 (2016), 1603.07321.
- [13] S.-R. Chen, H.-Y. Schive, and T. Chiueh, *Mon. Not. R. Astron. Soc.* **468**, 1338 (2017), 1606.09030.
- [14] V. H. Robles, J. S. Bullock, and M. Boylan-Kolchin, *Mon. Not. R. Astron. Soc.* **483**, 289 (2019), 1807.06018.
- [15] T. Bernal, L. M. Fernández-Hernández, T. Matos, and M. A. Rodríguez-Meza, *Mon. Not. R. Astron. Soc.* **475**, 1447 (2018), 1701.00912.
- [16] N. Bar, D. Blas, K. Blum, and S. Sibiryakov, *Phys. Rev. D* **98**, 083027 (2018), 1805.00122.
- [17] N. C. Amorisco and A. Loeb, *arXiv e-prints*, arXiv:1808.00464 (2018), 1808.00464.
- [18] B. Bar-Or, J.-B. Fouvry, and S. Tremaine, *Astrophys. J.* **871**, 28 (2019), 1809.07673.
- [19] B. V. Church, P. Mocz, and J. P. Ostriker, *Mon. Not. R. Astron. Soc.* **485**, 2861 (2019), 1809.04744.
- [20] A. A. El-Zant, J. Freundlich, F. Combes, and A. Halle, *Mon. Not. R. Astron. Soc.* **492**, 877 (2020), 1908.09061.
- [21] I. De Martino *et al.*, *Phys. Rev. Lett.* **119**, 221103 (2017), 1705.04367.
- [22] T. D. Brandt, *Astrophys. J. Lett.* **824**, L31 (2016), 1605.03665.
- [23] D. J. E. Marsh and J. C. Niemeyer, *Phys. Rev. Lett.* **123**, 051103 (2019), 1810.08543.
- [24] T. S. Li *et al.*, *Astrophys. J.* **838**, 8 (2017), 1611.05052.
- [25] D. Crnojević *et al.*, *Astrophys. J. Lett.* **824**, L14 (2016), 1604.08590.
- [26] H.-Y. Schive *et al.*, *Mon. Not. R. Astron. Soc.* **481**, 4815 (2018), 1712.07070.
- [27] S.-C. Lin, H.-Y. Schive, S.-K. Wong, and T. Chiueh, *Phys. Rev. D* **97**, 103523 (2018), 1801.02320.

- [28] T. K. Fritz *et al.*, *Astron. Astrophys.***619**, A103 (2018), 1805.00908.
- [29] A. B. Pace and T. S. Li, *Astrophys. J.* **875**, 77 (2019), 1806.02345.
- [30] V. Lora, J. Magaña, A. Bernal, F. J. Sánchez-Salcedo, and E. K. Grebel, *J. Cosmol. Astropart. Phys.***2012**, 011 (2012), 1110.2684.
- [31] L. Lancaster *et al.*, *J. Cosmol. Astropart. Phys.***2020**, 001 (2020), 1909.06381.
- [32] I. De Martino, T. Broadhurst, S. H. Henry Tye, T. Chiueh, and H.-Y. Schive, *Physics of the Dark Universe* **28**, 100503 (2020), 1807.08153.
- [33] N. Bar, K. Blum, J. Eby, and R. Sato, *Phys. Rev. D* **99**, 103020 (2019), 1903.03402.
- [34] Z. Li, J. Shen, and H.-Y. Schive, *Astrophys. J.* **889**, 88 (2020), 2001.00318.